
Supporting Information

Activating Copper for Electrocatalytic CO₂ Reduction to Formate via Molecular Interactions

Zixu Tao^{1,2}, Zishan Wu^{1,2}, Yueshen Wu^{1,2}, Hailiang Wang^{*1,2}

¹Department of Chemistry, Yale University, New Haven, Connecticut 06520, United States

²Energy Sciences Institute, Yale University, West Haven, Connecticut 06516, United States

*Corresponding author

Email address: hailiang.wang@yale.edu

Synthesis of CuO nanoparticles

300 μ L of glacial acetic acid was added to 90 mL of Cu(NO₃)₂ aqueous solution (0.02 M) and then heated in a 100 °C oil bath for 20 min. Next, 700 μ L of aqueous NaOH (25 wt.%) was quickly injected under vigorous magnetic stirring. The reaction was allowed to proceed for 20 min, after which it was cooled down in an ice water mixture. The product was collected by centrifugation at 14000 RPM for 10 min and washed with a 1:3:4 water/ethanol/acetone mixture once. It was then re-dispersed in water and freeze-dried.

Structural characterization

X-ray diffraction (XRD) data were collected on a Rigaku SmartLab X-ray diffractometer with a Cu target (154 pm wavelength) operated at 44 kV and 40 mA. X-ray photoelectron spectroscopy (XPS) was performed on a PHI VersaProbe II X-ray photoelectron spectrometer with an Al K _{α} target (1486.7 eV). The energy scale for all spectra was calibrated by fixing the C 1s peak at 284.8 eV. To perform XPS, the post-electrolysis electrode was rinsed with Ar-purged water and ethanol successively and transferred into the spectrometer via an air-tight sample transfer vessel. Scanning electron microscopy (SEM) was performed on a Hitachi SU8230 scanning electron microscope.

Electrochemical measurements

CO₂ reduction measurements were carried out in a home-made three-electrode H-cell separated by an anion exchange membrane (Selemion DSV). The data were recorded by a Bio-Logic VMP3

electrochemistry workstation. The electrolyte was a 0.5 M KHCO_3 aqueous solution which had been electrochemically purified by maintaining a current of 150 μA between two parallelly placed Ti sheets in the electrolyte for 24 h with magnetic stirring. An ethanol suspension containing 1 mg mL^{-1} of CuO nanoparticles was homogenized by sonication, and then the working electrode was prepared by drop-casting 200 μL of this suspension on a 1 cm^2 area of carbon fiber paper (Toray-030, 30% polytetrafluoroethylene). The final mass loading of CuO nanoparticles was 0.2 mg cm^{-2} . The reference electrode was Ag/AgCl (saturated KCl) and it was placed close to the working electrode in the cathodic compartment of the H-cell; the counter electrode was a graphite rod placed in the anodic compartment. Potentials were calibrated and reported to the RHE scale unless otherwise specified, and 100% iR compensation was applied during every CO_2 reduction measurement. Electrochemical impedance spectroscopy was used to determine the resistance. The working electrode potential was set to 0.1 V vs. RHE, and the frequency was scanned from 200 kHz to 100 Hz. Afterwards, the resistance was determined as the intersection between the Nyquist plot and the x-axis (i.e. real impedance). The resistance value with 0.5 M KHCO_3 as electrolyte was typically 3~4 Ω .

A galvanostatic procedure was conducted prior to the CO_2 reduction to reduce the CuO nanoparticles in the purified 0.5 M KHCO_3 electrolyte. Specifically, a 1 mA cathodic current was applied on the working electrode for 15 min under continuous Ar purging in the cathodic compartment. The total charge passed was 1.8 times as much as needed to reduce the 0.2 mg of CuO on the electrode, to ensure that the CuO nanoparticles were fully reduced to Cu after this step.

For the measurements with CTAB and other additives, 100 μL of 20 mM CTAB (or other additives) aqueous solution was added to 12 g of the electrolyte, yielding a concentration of approximately 0.167 mM unless otherwise specified.

CO_2 was bubbled into the electrolyte continuously at a flow rate of 20 sccm during the CO_2 reduction process. Gas products were analyzed by a gas chromatograph. The gas chromatograph (MG#5, SRI Instruments) was operated with Ar as the carrier gas. The quantification was calibrated by running standard gaseous samples containing known amounts of H_2 , CO, CH_4 and C_2H_4 . Liquid products were

quantified by conducting ^1H -nuclear magnetic resonance (^1H -NMR) spectroscopy under the water suppression mode. ^1H -NMR spectra were collected on a Bruker 400 MHz Broadband Probe NMR spectrometer. 450 μL of post-electrolysis electrolyte extracted from the cathodic compartment was mixed with 50 μL of an internal standard solution containing 50 mM of potassium benzoate and 10 mM of dimethyl sulfoxide in D_2O . By establishing a calibration curve (Figure S13) from standard formic acid solutions, formate, which was the only liquid product from CO_2 reduction in this study, could be quantified (typically within the 0.5 mM \sim 0.2 M range).

Electrochemical CO_2 reduction performance tests were performed in a potentiostatic mode, i.e. carried out by holding the working electrode at a given potential for 1 h. 3 parallel electrolysis runs were performed at each potential to obtain the average values and standard deviations.

Relative surface area was measured from the non-Faradaic charge adsorption process. In the same electrolyte and cell configuration after 1 h of electrolysis, cyclic voltammetry was performed in the 0 \sim 0.2 V range, where no Faradaic process was observed. The scan rate was varied in the range between 20 and 100 mV s^{-1} . After plotting the current density at 0.2 V vs. the scan rate, relative surface area (in the unit of mF cm^{-2}) was derived from the slope.

In-situ Raman spectroscopy measurements

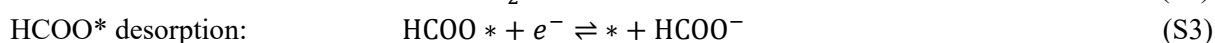
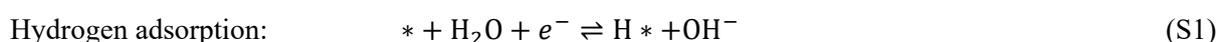
A home-made H-shape Raman cell separated by an anion exchange membrane was used to perform Raman spectroscopy under electrochemical CO_2 reduction conditions (Figure S2). The reference electrode was Ag/AgCl (saturated KCl) placed in the cathodic compartment; the counter electrode was a graphite rod placed in the anodic compartment. The working electrode was a piece of Ti foil loaded with CuO nanoparticles. A desired gas (CO_2 or Ar) was continuously bubbled into the electrolyte near the working electrode. The electrolysis was controlled by a Bio-Logic SP150 electrochemistry workstation.

Raman spectroscopy was performed on a HORIBA LabRAM HR Evolution Raman microscope with a 633 nm laser and an OLYMPUS LUMPLFLN60XW water-immersion objective lens. Raman spectra

were taken under potentiostatic conditions, and the laser spot was placed at a fixed position for recording one set of spectra at different electrode potentials. The data were collected and processed by a bundled software (LabSpec 6). Each set of Raman spectra were collected at a single spot, plotted using the same intensity scale, and displayed in a single graph. The intensity scale was varied across different sets of spectra to ensure the spectral features are clearly shown.

Tafel analysis

The Tafel slopes measured in Figure S11a could be explained with a 3-step mechanism of CO₂ reduction to formate:



We calculated the Tafel slope to be 120 mV dec⁻¹ under the condition of high H* coverage and (S3) being the rate-limiting step, which is very close to our measured value of 112 mV dec⁻¹.

Supplementary display items

Table S1. Performance comparison of Cu-based electrocatalysts for CO₂ reduction to formate.

Samples	Electrolyte	FE (formate)	Potential (vs. RHE)	j_{formate}	Ref.
Cu-CTAB	0.5 M KHCO₃	82.3%	-0.5 V	2.48 mA cm⁻²	This work
Sulfur-modified Cu	0.1 M KHCO ₃	80%	-0.8 V	8 mA cm ⁻²	1
AC-CuS _x	0.1 M KHCO ₃	75%	-0.85 V	5 mA cm ⁻²	2
Thick Cu ₂ O films	0.5 M NaHCO ₃	33%	-0.5 V	0.89 mA cm ⁻²	3
Cu nanofoams	0.1 M KHCO ₃	37%	-0.9 V	3.7 mA cm ⁻²	4
Cu-CDots	0.5 M KHCO ₃	68%	-0.7 V	2.9 mA cm ⁻²	5
Porous dendric Cu	[EMIM](BF ₄)/H ₂ O (92:8 v/v)	83%	-0.983 V	4.3 mA cm ⁻²	6
Polished Cu with CTAB	0.1 M NaHCO ₃	48%	-0.6 V	0.67 mA cm ⁻²	7
Cu-hydride nanoclusters	0.1 M KHCO ₃ + 0.4 M KCl	89%	-0.54 V	1.4 mA cm ⁻²	8
Sulfur-doped Cu	0.1 M KHCO ₃	74%	-0.8 V	10.7 mA cm ⁻²	9
CuODS	0.1 M KHCO ₃	76.5%	-0.9 V	12.3 mA cm ⁻²	10

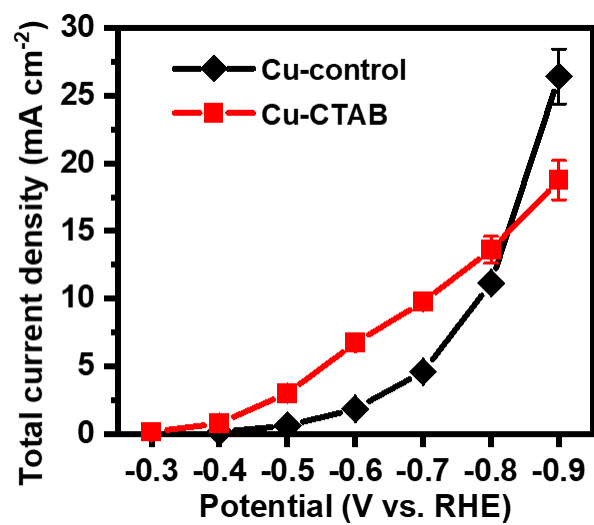


Figure S1. Potential-dependent total current density for Cu-control and Cu-CTAB in CO₂-saturated 0.5 M aqueous KHCO₃.

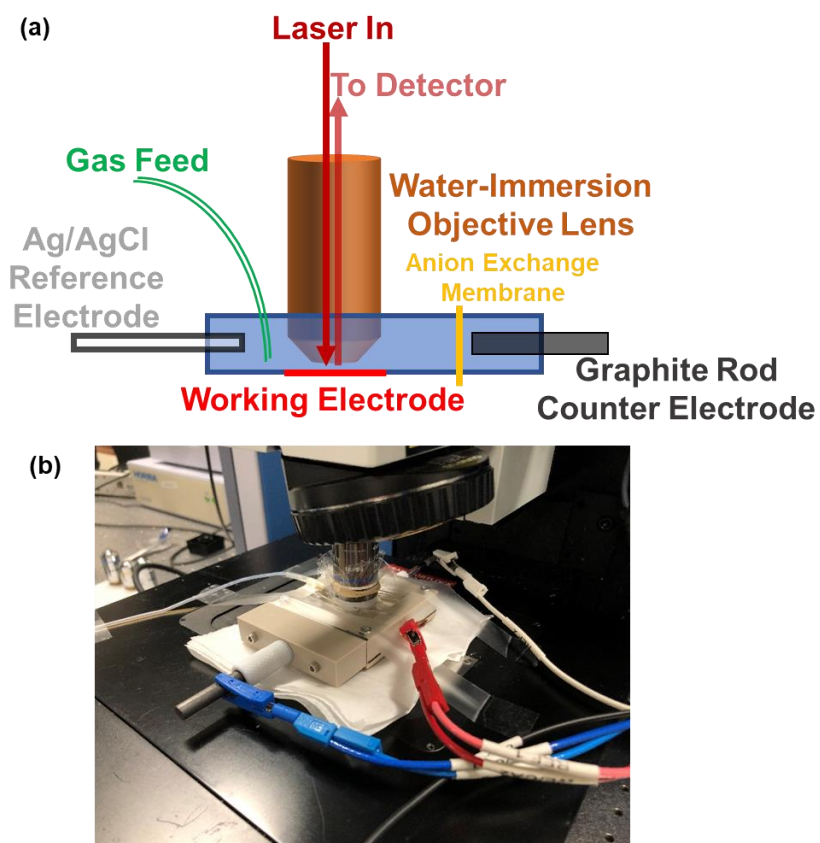


Figure S2. (a) Schematic illustration and (b) photograph of the system setup to perform in-situ Raman spectroscopy under electrochemical CO₂ reduction conditions.

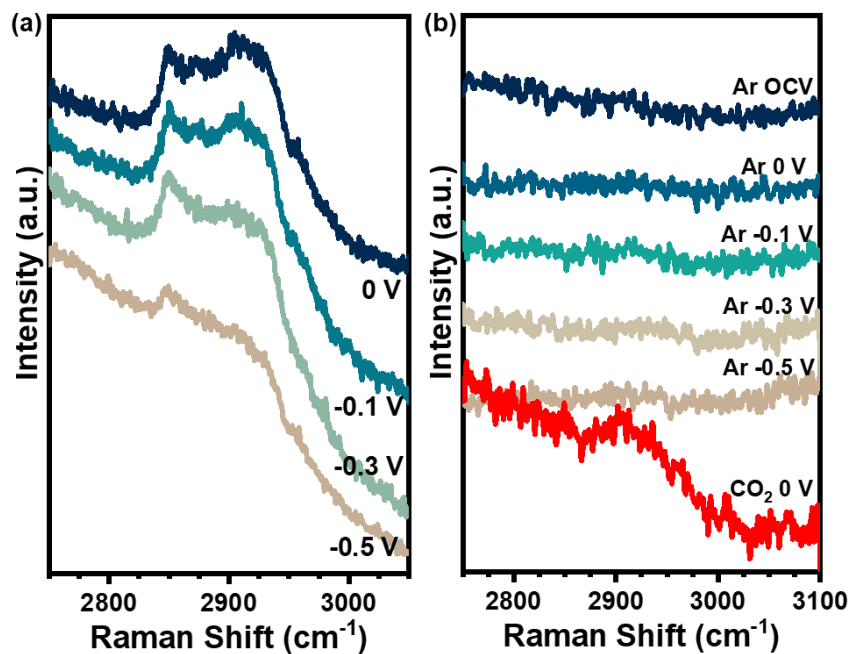


Figure S3. In-situ Raman spectra for Cu-control under different conditions. (a) Ar-purged 0.5 M KHCO₃ + 10 mM HCOOK; (b) 0.1 M KClO₄. OCV stands for open circuit voltage.

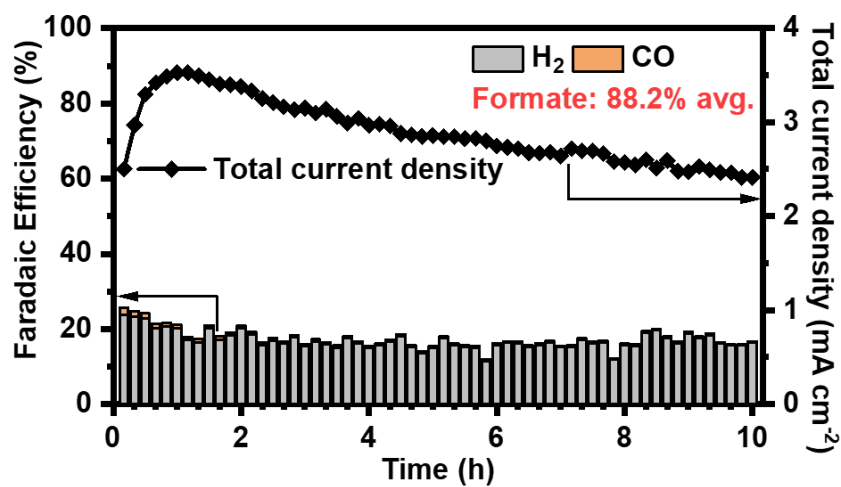


Figure S4. 10 h stability test for CO₂ reduction catalyzed by Cu-CTAB at -0.5 V. The average formate FE was quantified after the electrolysis.

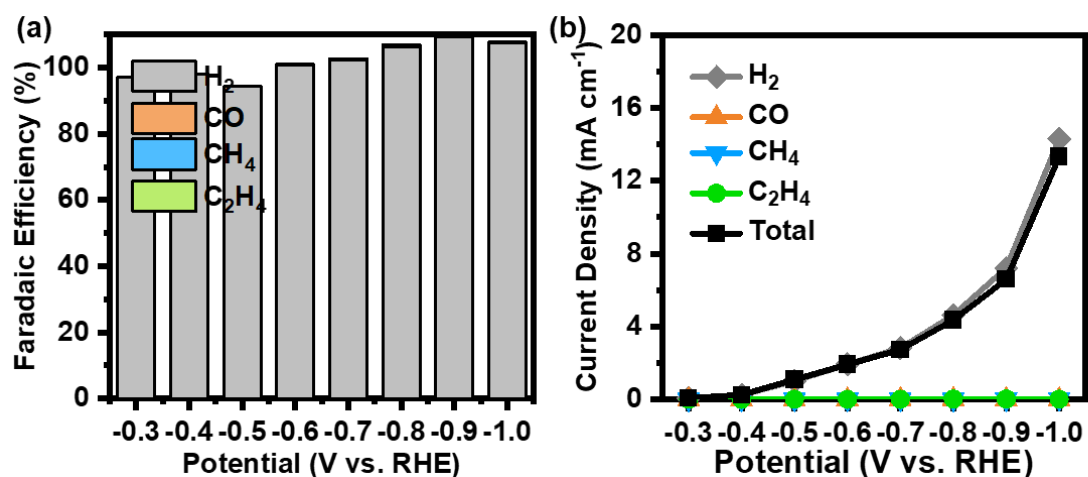


Figure S5. Potential-dependent CO₂ reduction performance for Cu-CTAB in Ar-purged 0.5 M KHCO₃: (a) Faradaic efficiency and (b) partial current densities for different products.

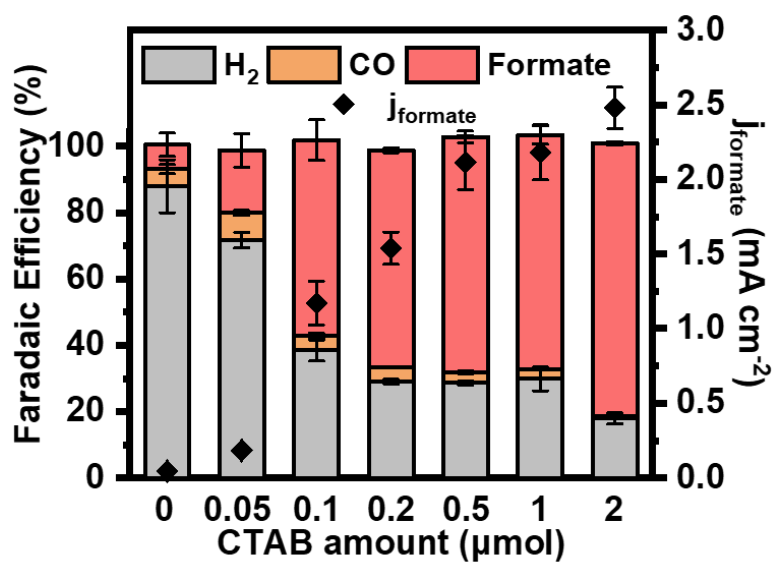


Figure S6. CO₂ reduction performance (FE shown by the columns and current density indicated by the diamond dots) at -0.5 V for Cu-CTAB with different CTAB concentrations. The horizontal axis shows the amount of CTAB added into 12 g of 0.5 M KHCO₃ electrolyte to reach different concentrations, for example, 2 μmol to make 0.167 mM.

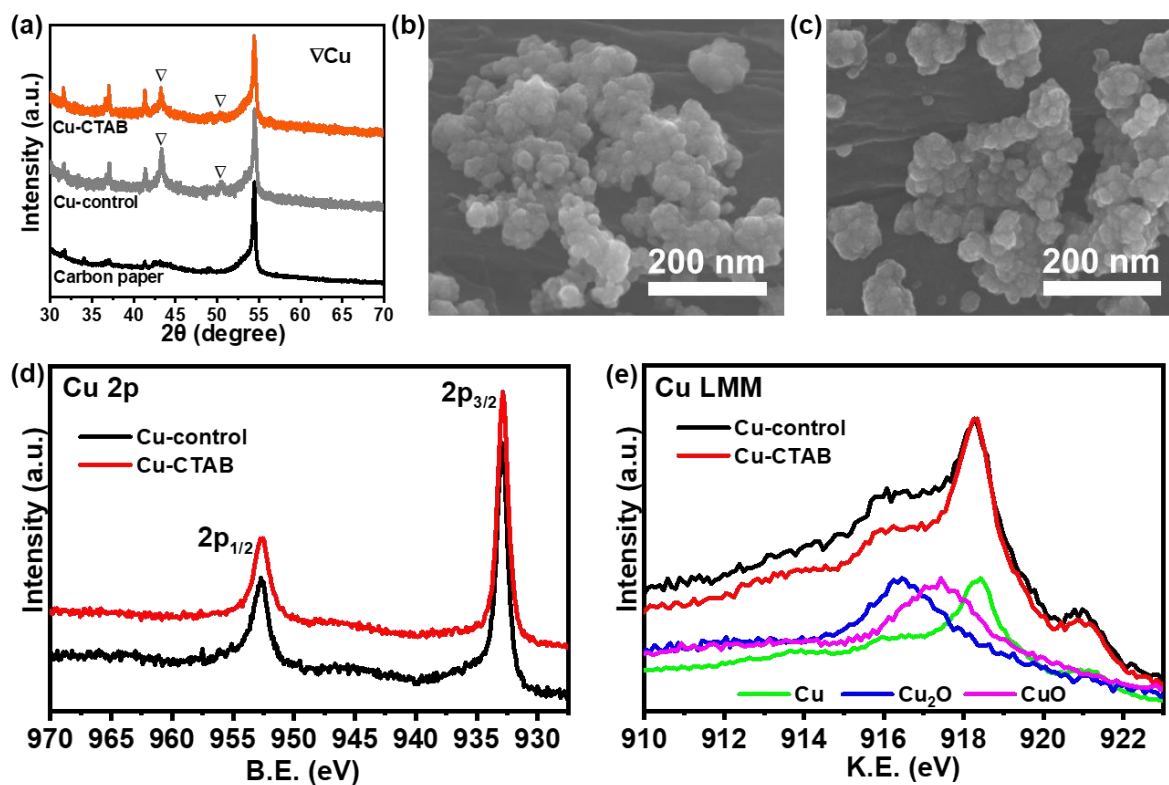


Figure S7. Structural characterization of Cu-control and Cu-CTAB. (a) XRD diagrams. (b-c) SEM images of (b) Cu-control and (c) Cu-CTAB. (d) Cu 2p XPS spectra and (e) Cu LMM Auger spectra.

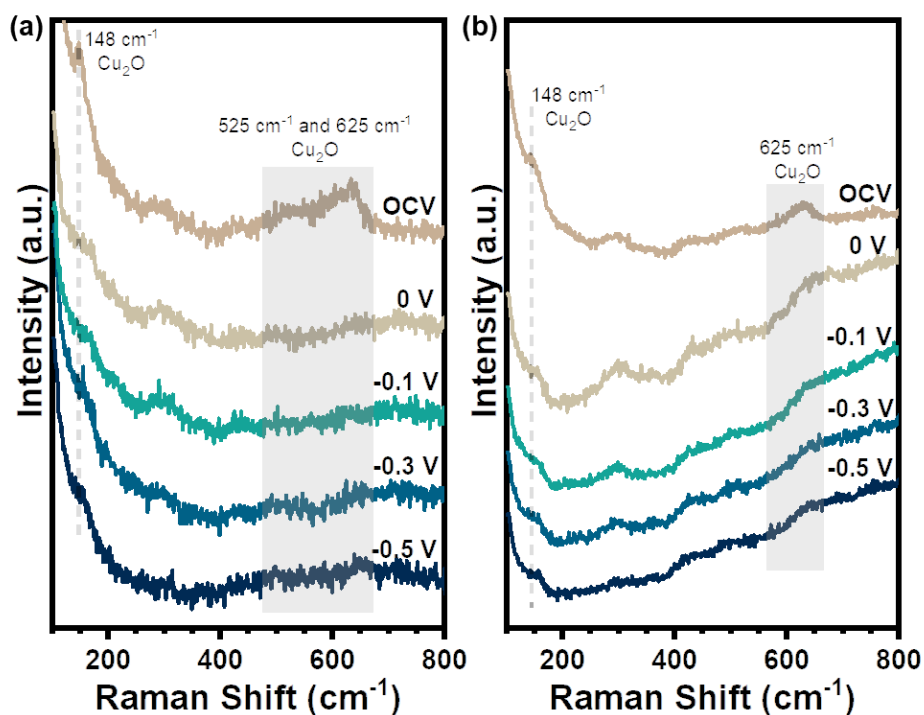


Figure S8. In-situ Raman spectra for (a) Cu-control and (b) Cu-CTAB tested in CO_2 -purged 0.5 M KHCO_3 .

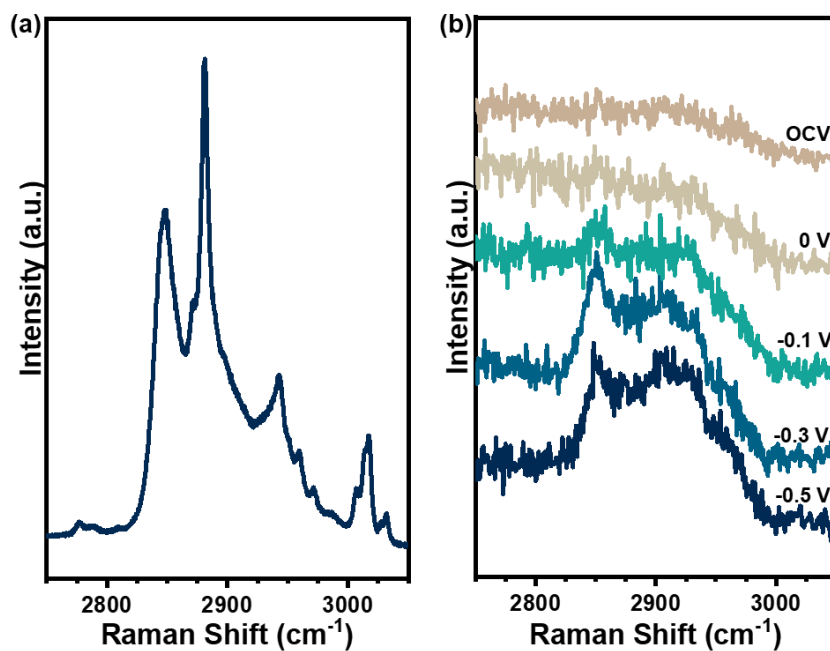


Figure S9. (a) Raman spectrum of CTAB powder. (b) In-situ Raman spectra for Cu-CTAB in Ar-purged 0.5 M KHCO₃.

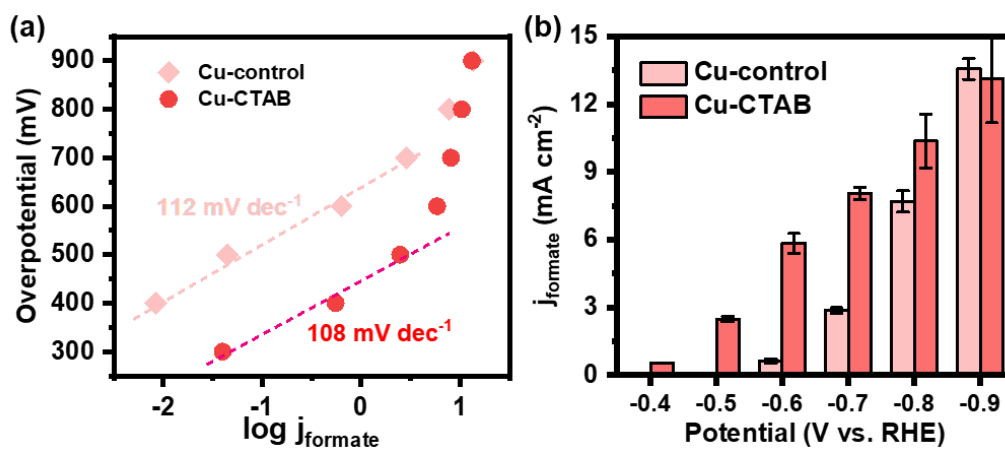


Figure S10. (a) Tafel plots and (b) partial current density of CO₂-to-formate reduction for Cu-control and Cu-CTAB.

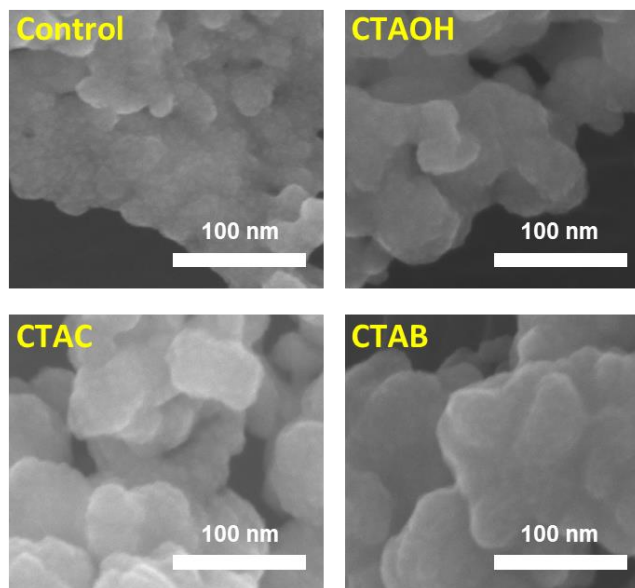


Figure S11. SEM images of Cu after 1 h CO₂ reduction electrolysis at -0.5 V with cetyltrimethylammonium salts consisting of different anions.

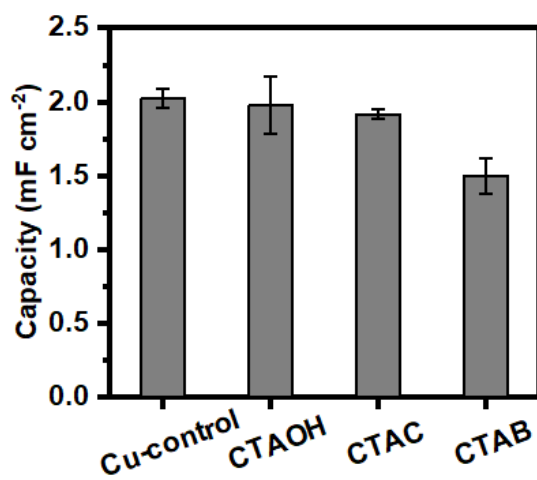


Figure S12. Relative surface area of Cu after 1 h CO₂ reduction electrolysis at -0.5 V with cetyltrimethylammonium salts consisting of different anions.

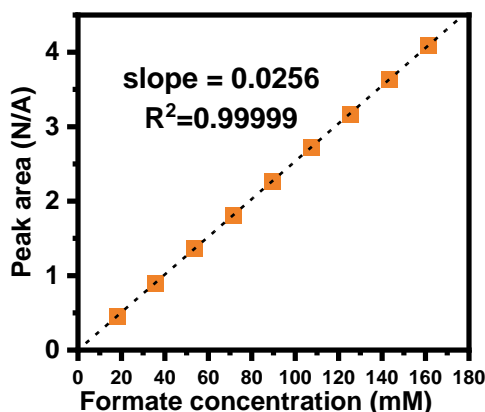


Figure S13. Calibration curve for quantifying formate concentration by $^1\text{H-NMR}$ with 50 mM of potassium benzoate as the internal standard. The formate peak area was integrated with the $\delta_{7.83\text{ppm}}$ benzoate peak normalized to 1.

References

1. Shinagawa, T.; Larrazabal, G. O.; Martin, A. J.; Krumeich, F.; Perez-Ramirez, J., Sulfur-Modified Copper Catalysts for the Electrochemical Reduction of Carbon Dioxide to Formate. *ACS Catal.* **2018**, 8 (2), 837-844.
2. Deng, Y.; Huang, Y.; Ren, D.; Handoko, A. D.; Seh, Z. W.; Hirunsit, P.; Yeo, B. S., On the Role of Sulfur for the Selective Electrochemical Reduction of CO_2 to Formate on CuS_x Catalysts. *ACS Appl. Mater. Interfaces* **2018**, 10 (34), 28572-28581.
3. Li, C. W.; Kanan, M. W., CO_2 Reduction at Low Overpotential on Cu Electrodes Resulting from the Reduction of Thick Cu_2O Films. *J. Am. Chem. Soc.* **2012**, 134 (17), 7231-7234.
4. Sen, S.; Liu, D.; Palmore, G. T. R., Electrochemical Reduction of CO_2 at Copper Nanofoams. *ACS Catal.* **2014**, 4 (9), 3091-3095.
5. Guo, S.; Zhao, S.; Gao, J.; Zhu, C.; Wu, X.; Fu, Y.; Huang, H.; Liu, Y.; Kang, Z., Cu-CDots Nanocorals as Electrocatalyst for Highly Efficient CO_2 Reduction to Formate. *Nanoscale* **2017**, 9 (1), 298-304.
6. Huan, T. N.; Simon, P.; Rouse, G.; Génois, I.; Artero, V.; Fontecave, M., Porous Dendritic Copper: an Electrocatalyst for Highly Selective CO_2 Reduction to Formate in Water/Ionic Liquid Electrolyte. *Chemical Science* **2017**, 8 (1), 742-747.
7. Banerjee, S.; Han, X.; Thoi, V. S., Modulating the Electrode–Electrolyte Interface with Cationic Surfactants in Carbon Dioxide Reduction. *ACS Catal.* **2019**, 9 (6), 5631-5637.
8. Tang, Q.; Lee, Y.; Li, D. Y.; Choi, W.; Liu, C. W.; Lee, D.; Jiang, D. E., Lattice-Hydride Mechanism in Electrocatalytic CO_2 Reduction by Structurally Precise Copper-Hydride Nanoclusters. *J. Am. Chem. Soc.* **2017**, 139 (28), 9728-9736.
9. Huang, Y.; Deng, Y.; Handoko, A. D.; Goh, G. K. L.; Yeo, B. S., Rational Design of Sulfur-Doped Copper Catalysts for the Selective Electroreduction of Carbon Dioxide to Formate. *ChemSusChem* **2018**, 11 (1), 320-326.
10. Pan, Z.; Wang, K.; Ye, K.; Wang, Y.; Su, H.-Y.; Hu, B.; Xiao, J.; Yu, T.; Wang, Y.; Song, S., Intermediate Adsorption States Switch to Selectively Catalyze Electrochemical CO_2 Reduction. *ACS Catal.* **2020**, 10 (6), 3871-3880.